

## Optimizing Numerical Modelling for In-Plane Response of Clay and Calcium Silicate Masonry through Data-Informed Semi-Automation

Abide Aşıkoğlu<sup>i</sup>, Paul Korswagen<sup>ii</sup>, and Jan Rots<sup>iii</sup>

### ABSTRACT

This study presents a semi-automated, data-informed framework for selecting parameter-consistent numerical models to approximate the in-plane behaviour of clay and calcium silicate masonry walls. A comprehensive experimental campaign has been executed on full-scale unreinforced calcium silicate and clay masonry walls at Delft University of Technology. The in-plane response of these walls was evaluated based on stiffness, strength, damage intensity at equivalent drift levels, and the overall impact of the damage. The findings indicate that unreinforced calcium silicate masonry walls are more prone to damage through the brick units, while cracks in unreinforced clay masonry walls predominantly align with mortar joints. Calcium silicate walls tend to develop larger and more prominent cracks, often requiring the replacement of individual bricks for a complete repair. In contrast, the damage in clay walls is typically easier to address through repointing of mortar joints. A parametric finite element analysis was performed to investigate these failure mechanisms, systematically varying input parameters to generate 3,456 numerical simulations. Each model permutation was evaluated to select models that closely approximate observed experimental responses. Unlike conventional calibration methods, this framework systematically explores possible combinations of input and output parameters to identify numerical models that replicate key structural behaviours. The preliminary results demonstrate that multiple parameter combinations can yield numerical responses closely matching experimental observations, providing a structured approach for improving masonry modelling practices.

### KEYWORDS

Data-informed numerical model selection, semi-automation, parametric analysis, unreinforced calcium silicate and clay masonry, in-plane behaviour, and numerical-experimental agreement.

---

<sup>i</sup> Postdoc, Delft University of Technology, Delft, The Netherlands, a.ashikoglu@tudelft.nl

<sup>ii</sup> Assistant Professor, Delft University of Technology, Delft, The Netherlands, p.a.korswageneguren@tudelft.nl

<sup>iii</sup> Full Professor, Delft University of Technology, Delft, The Netherlands, j.g.rots@tudelft.nl

## INTRODUCTION

The numerical simulation of masonry structures plays a crucial role in understanding their complex mechanical behaviour under various loading conditions. Numerous modelling approaches that consider the nonlinear nature of masonry have been developed [1], and both nonlinear static and dynamic analysis procedures can be performed. Consequently, seismic design and assessment regulations have evolved into a performance-based methodology. However, the selection of the modelling approach, modelling assumptions, and analysis techniques is just one of the new challenges that this improvement has introduced [2]. Existing research on benchmark studies of masonry buildings highlights significant variability in results. A key factor contributing to these discrepancies is identified as strong user dependency in modelling decisions, including the selection of modelling strategies, material properties, boundary conditions, load representations, and interpretation of outputs [2–6]. Nevertheless, even if similar assumptions for materials are adopted, studies show significant variability in results among modelling approaches. This variability raises concerns regarding the reliability and consistency of numerical simulations. Cattari and Magenes (2002) [4] suggest that engineering judgment and expertise are crucial in obtaining reliable results, yet they also highlight the need for more standardized and systematic approaches to reduce subjectivity. Given the inherent variability in material properties and structural responses, selecting appropriate model parameters is essential for ensuring reliable numerical predictions. Traditional model calibration techniques often rely on iterative manual adjustments, which can be time-consuming and highly dependent on user expertise.

To address these challenges, this study proposes a data-informed approach for selecting parameter-consistent numerical models that best approximate experimental observations. Rather than directly optimizing model parameters, this method systematically evaluates a pool of numerical simulations to identify those exhibiting the highest experimental agreement, improving the reliability of numerical analysis. First, a broad set of numerical models is generated through a systematic parametric analysis. Then, the outputs from the pool of numerical simulations are evaluated to determine those with the highest experimental agreement. Unlike conventional calibration, this approach does not aim for a perfect match but rather prioritizes models that best approximate experimental observations, accounting for multiple input and output parameters. Moreover, unlike fully automated machine learning-based calibration techniques, this strategy retains user control and interpretability, allowing analysts to guide the process while minimizing biases associated with manual or automatic tuning. This semi-automated framework enhances reliability by reducing subjectivity in model selection while balancing computational efficiency and accuracy.

## TU DELFT IN-PLANE MASONRY WALL TESTS

A comprehensive experimental campaign has been executed on full-scale unreinforced calcium silicate and clay masonry walls at Delft University of Technology. The in-plane response of these walls was evaluated based on stiffness, strength, damage intensity at equivalent drift levels, and the overall impact of the damage. The present paper focuses on two identical full-scale masonry walls that were tested under in-plane cyclic loading with a constant pre-compression stress of 0.12 MPa. Each single-wythe wall measured approximately 3.1 m in width and 2.7 m in height. Both wall types were constructed with a cementitious general mortar, with a thickness of 10 mm. A window opening was positioned asymmetrically, as seen in Figure 1. The walls were fixed to a base steel beam, while the top steel beam located at the top of the walls was free to rotate and displace in its plane. This configuration is aimed at replicating a cantilever boundary condition. For further details of the experimental setup and results, the reader is referred to [7,8].

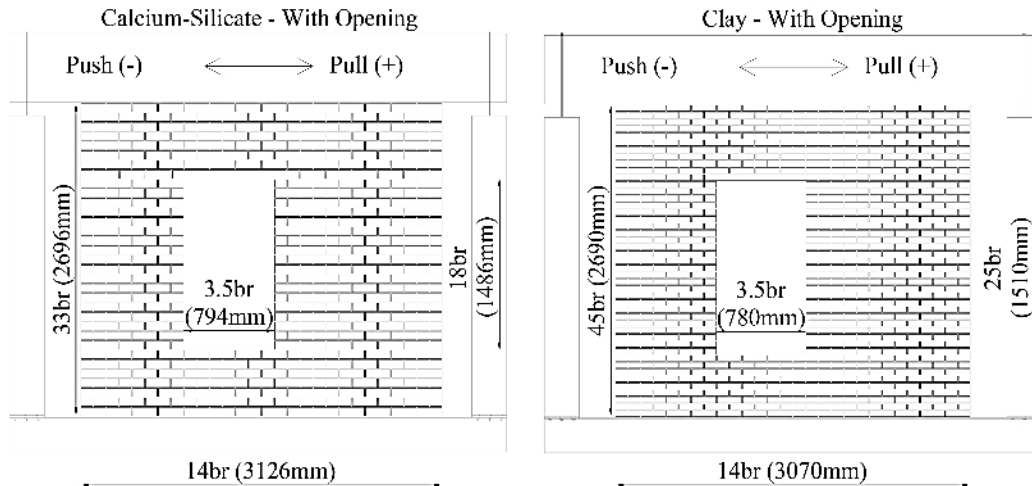


**Figure 1: Geometry of the unreinforced Calcium-Silicate and Clay masonry walls [8]**

Table 1 summarises the main differences between the two wall types in terms of stiffness, strength, damage behaviour, crack patterns, and failure mechanisms. The results show that calcium silicate masonry walls are more likely to develop cracks through the bricks, while cracks in clay walls mostly follow the mortar joints. Calcium silicate walls tend to develop larger and more visible cracks, often requiring brick replacement for repairs. Damage in clay walls is generally easier to address through repointing mortar joints. Korswagen et al. 2020 [7] states that calcium silicate bricks form a stronger bond with cement mortar, while the bricks themselves are weaker but stiffer. The relative stiffness and brittleness of the calcium silicate bricks are more likely to crack within the unit rather than at the mortar joints. It is expected that certain combinations of material properties may influence the failure type, however, further research is needed.

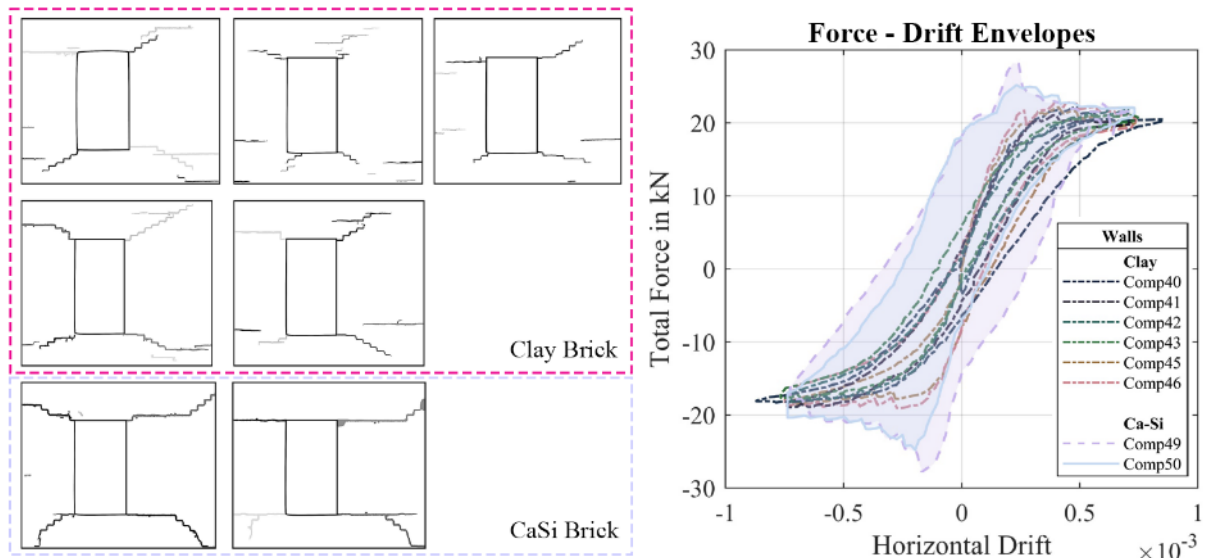


**Figure 2: Comparison of cumulative crack patterns of unreinforced Clay and Calcium-Silicate walls (left) and comparison of absolute envelopes between similar Clay walls and two Calcium-Silicate walls (right) [7]**

**Table 1: Comparison between the Calcium-Silicate and Clay URM Walls. Adapted from [7]**

Response	Calcium-Silicate URM Walls	Clay URM Walls
Stiffness	Stiffer	Less stiff
Strength	Higher strength in both positive and negative directions	Lower strength in comparison.
Damage at similar drift values	More damage, with higher hysteresis energy	Less damage, with lower hysteresis energy
Strength degradation	Observed	Relatively low
Crack patterns	Fewer and larger cracks propagating horizontally, diagonally, and vertically	More numerous individual cracks, predominantly diagonal, especially around window corners
Brick splitting	Observed	Not observed
Failure mechanisms	Brittle	Relatively more ductile

## DATA-INFORMED SEMI-AUTOMATED NUMERICAL ANALYSES

This study proposes a data-informed, semi-automated framework for selecting parameter-consistent numerical models that best approximate experimental observations. The underlying hypothesis of the proposed approach is that multiple combinations of parameters can achieve responses that closely align with the same experimental observations. The terminology that is used within the scope of the proposed approach is given below.

- *Semi-automated*: Refers to a process that integrates automated computational techniques with human input or oversight. While automation helps the analysts to reduce manual effort and expand the range of possible cases, human input or oversight plays a key role in decision-making to guide the process, ensuring physically meaningful results and minimizing biases.
- *Data-informed model selection*: Involves using experimental data to guide model selection, while incorporating human judgment or other considerations in the decision-making process. This process differs from data-driven, which is entirely based on data in an automated way.
- *Parameter-consistent model*: Refers to numerical models which have consistent parameters within a predefined range that aligns with realistic material properties. This ensures the models reflect plausible structural behaviour, eliminating unrealistic parameter sets which could be obtained by full-automated machine learning methods. These models filter out unrealistic parameter sets while still allowing parameter variation.
- *Experimental agreement* refers to numerical responses that most closely approximate experimental observations.

## Methodology

The proposed methodology consists of four key stages, and a flowchart of the framework is illustrated in Figure 3. While some tasks follow a sequential dependency, others can be performed in parallel without a strict order. Nevertheless, the initial step of the method ultimately takes place in the Experimental phase, where a predefined test setup serves as a reference for guiding the numerical model development. This phase may involve conducting experiments or selecting a set of tests from an existing database. In the present paper, the experimental campaign including in-plane testing of calcium-silicate and clay brick walls is considered to assess their response and differences, as described previously. Within this scope, four tests on clay walls, namely Comp41, Comp43, Comp45, and Comp46, while two tests on CaSi walls, Comp49 and Comp50, were considered.

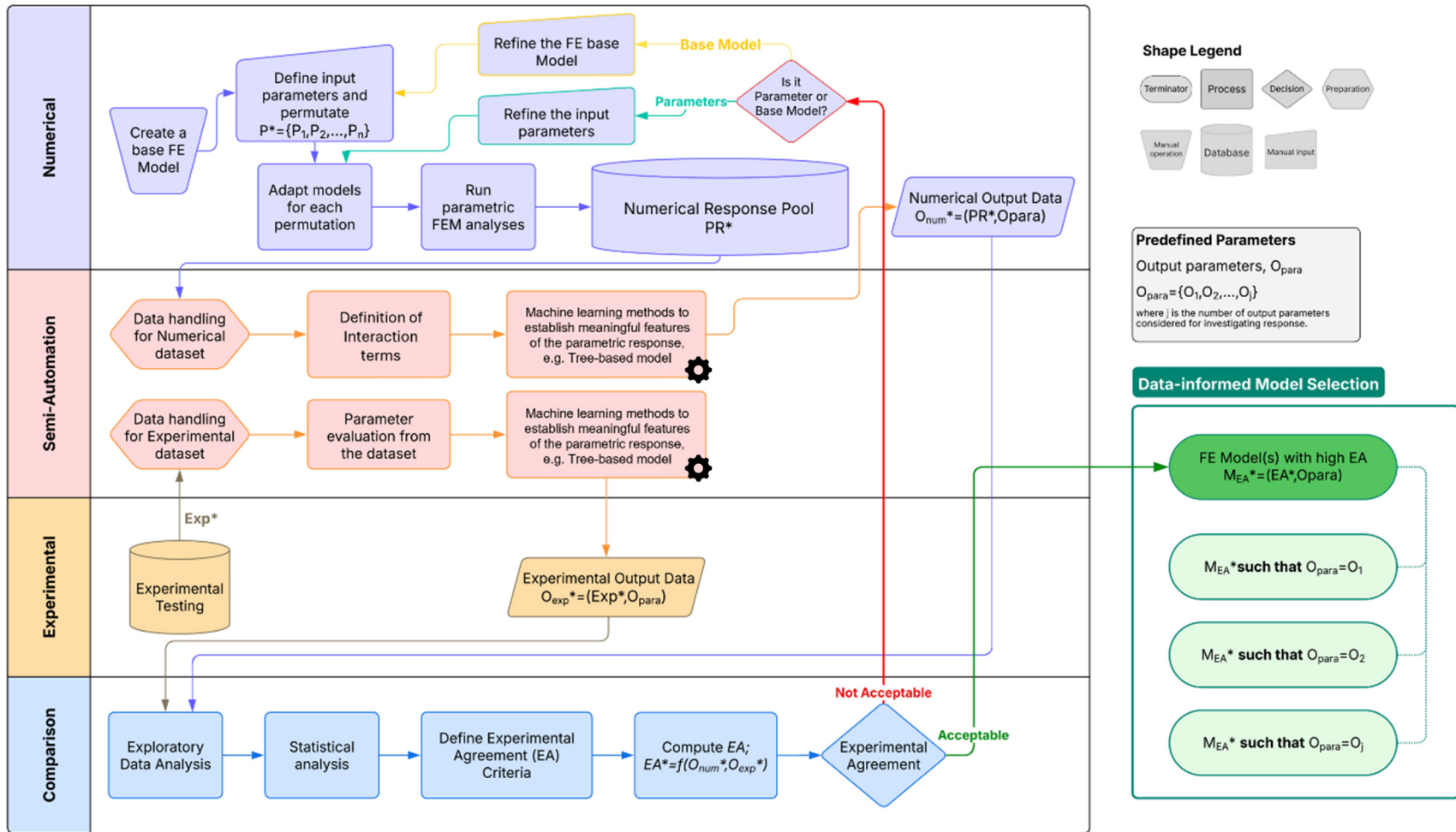
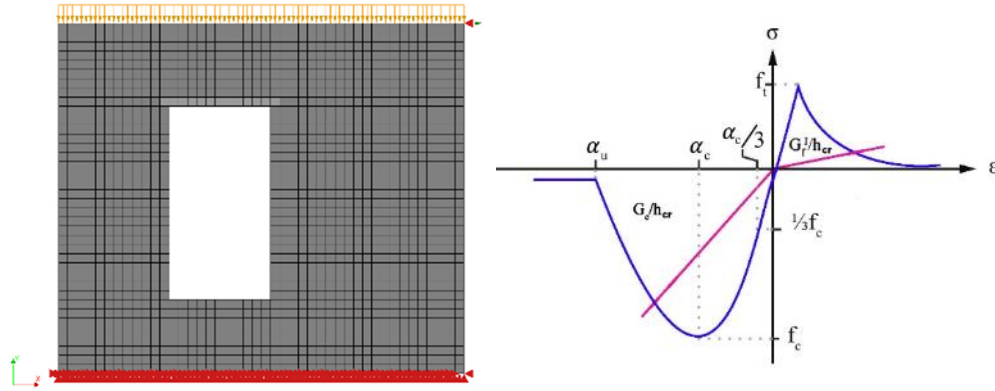


Figure 3: Flowchart of the proposed methodology

To this end, a continuum finite element approach was adopted in the present paper, and masonry walls were modelled using the macro-element approach in DIANA FEA [9]. The heterogeneous assemblage of mortar and bricks was smeared out into a homogenous anisotropic continuum, as shown in Figure 4. A two-dimensional continuum finite element (FE) model was constructed by using shell elements with an element type “CQ16M”, which is an eight-node quadrilateral isoparametric plane stress element. The constitutive material model was implemented through the Total Strain Crack Model (TSCM) [10] to simulate the material behaviour of both masonry materials. The TSCM follows the concept of hypo-elasticity in which the stress-strain relationship is defined based on the total accumulated strain, including both elastic and plastic deformations. The material may exhibit characteristics of nonlinear behaviour, such as strength and stiffness degradation; however, permanent deformation is not included in the stress-strain relationship, as illustrated in Figure 4. The tensile behaviour of the masonry was assumed to follow an exponential stress-strain relationship beyond the maximum tensile strength. For compression, a parabolic stress-strain relationship was defined for both the hardening and softening phases. TSCM integrates the stress-strain concept using two approaches, which are also considered in the present study, (i) coaxial concept or rotating crack model refers to evaluating the stress-strain relations in the principal directions of the strain vector, while (ii) fixed crack model evaluates stress-strain relations within the coordinate system that remains fixed even after cracking occurs [9]. Given the limitations of the TSCM on considering accumulated damage, monotonic load application was considered rather than cyclic. Therefore, nonlinear static analysis was performed only in the positive direction.



**Figure 4: FE model of the wall (left), constitutive model as TSCM [10] (right)**

Table 2 presents the input parameters used to permute the base FE model to perform the parametric analysis, along with their corresponding keywords, units, and range of values. Once the base FE model is created and input parameters are defined, an algorithm developed by the authors is used to permute these parameters, considering all possible combinations systematically, using MATLAB [11]. Accordingly, the total number of permutations is 3456. Each permutation is then implemented in the base FE model through an automated algorithm that generates \*.dat and \*.dcf files required to run analyses in DIANA FEA. Following the nonlinear analyses, the model responses from all permutations are collected into a dataset, referred to as the numerical response pool. The raw data is then pre-processed by extracting the relevant output parameters. To evaluate the experimental agreement of the numerical simulations, various output parameters ( $O_{para}$ ) are analysed for comparison. These parameters include, but are not limited to, peak force ( $F_{peak}$ ), displacement at peak force ( $d_{F_{peak}}$ ), maximum displacement ( $d_{max}$ ), force at maximum displacement ( $F_{d_{max}}$ ), elastic stiffness ( $k_e$ ), force at crack initiation ( $F_{cr}$ ), displacement at crack initiation ( $d_{cr}$ ), and post-crack displacement ratio ( $PCDR$ ).

**Table 2: Considered input parameters for permutation and parametric analysis**

Input parameters	Keywords	Units	Values
Young's Modulus	YOUNG	MPa	{2000, 2500, 3000, 4000, 5000, 5500, 7000, 9000}
Tensile Strength	TENSTR	MPa	{0.10, 0.20, 0.25, 0.50, 0.75, 1.00}
Poisson Ratio	POISON	-	{0.10, 0.15, 0.20}
Tensile Fracture Energy	GF1	N/mm	{0.005, 0.010, 0.012, 0.020}
Material Model	MATMDL	-	{TSCR}
Total Strain	TOTCRK	-	{Fixed, Rotating}
Compressive Strength	COMSTR	MPa	{5.00, 7.66, 12.00}

To understand the combined influence of multiple input parameters on the output, interaction terms are generated by multiplying these input parameters. In this case, Young's Modulus ( $E$ ), Tensile Strength ( $f_t$ ), Poisson Ratio ( $\nu$ ), Tensile Fracture Energy ( $G_{ft}$ ), and Compressive Strength ( $f_c$ ) are considered for all possible combinations of these parameters. While traditional correlation analysis captures individual parameter effects, it does not account for their interaction, where multiple parameters allow for acquiring nonlinear dependencies and higher-order effects. Accordingly, these terms are computed for the combination of 5 inputs by following the binomial coefficient ( $nchoosek$  function in MATLAB). Finally, the correlation coefficient between each interaction term and output parameter is calculated and presented in a matrix form, as depicted in Figure 5.

### Correlation Analysis and Tree-Based Model on Numerical Data: Preliminary Analysis

The correlation analysis showcases linear dependencies between input and output variables. Using interaction terms in the analysis introduces nonlinearity into the system. This enables investigating the influence of two or more input combinations on the output and whether they are more significant than their individual effects or not. The correlation matrix presented in Figure 5 shows the pairwise Pearson correlation coefficients between interaction terms and output variables. In this sense, if an interaction term has a stronger correlation with an output than its components, it confirms that combinations of features contribute more than the inputs alone. For example, in Figure 5, individual variables  $E$ ,  $f_t$ , and  $G_{ft}$  show a correlation of 0.60, 0.39, and 0.28 with  $F_{peak}$ , respectively. Their combined effect results in a higher correlation of 0.70, 0.62 or 0.74. This supports the hypothesis that interaction effects are non-trivial and crucial for accurate modelling. Having said that, interaction terms having a low correlation with the output variables do not indicate these terms are irrelevant; rather, their influence might be revealed through nonlinear models such as tree-based models. Thus, a Random Forest regression model was employed to evaluate the relative importance of interaction terms in predicting multiple output parameters to complement the correlation analysis. The number of input parameters considered is represented by ' $k$ ', ranging from one to combination of five parameters. For each output, a separate model was trained using the bagging method. The importance of each predictor was quantified by measuring the increase in prediction error when a predictor is randomly permuted. This approach provides an estimate of how much each input contributes to the response. The results are presented as a bar chart for each output parameter, as shown in Figure 5. Accordingly, a few key insights are compiled from these methods:

- Parameter combinations with low correlation but high feature importance may confirm a non-linear relationship.
- If both correlation and importance features are high, a strong linear effect may be confirmed, for instance, Young's Modulus.
- If both terms are low, the parameters may not be correlated with the output and can be eliminated.







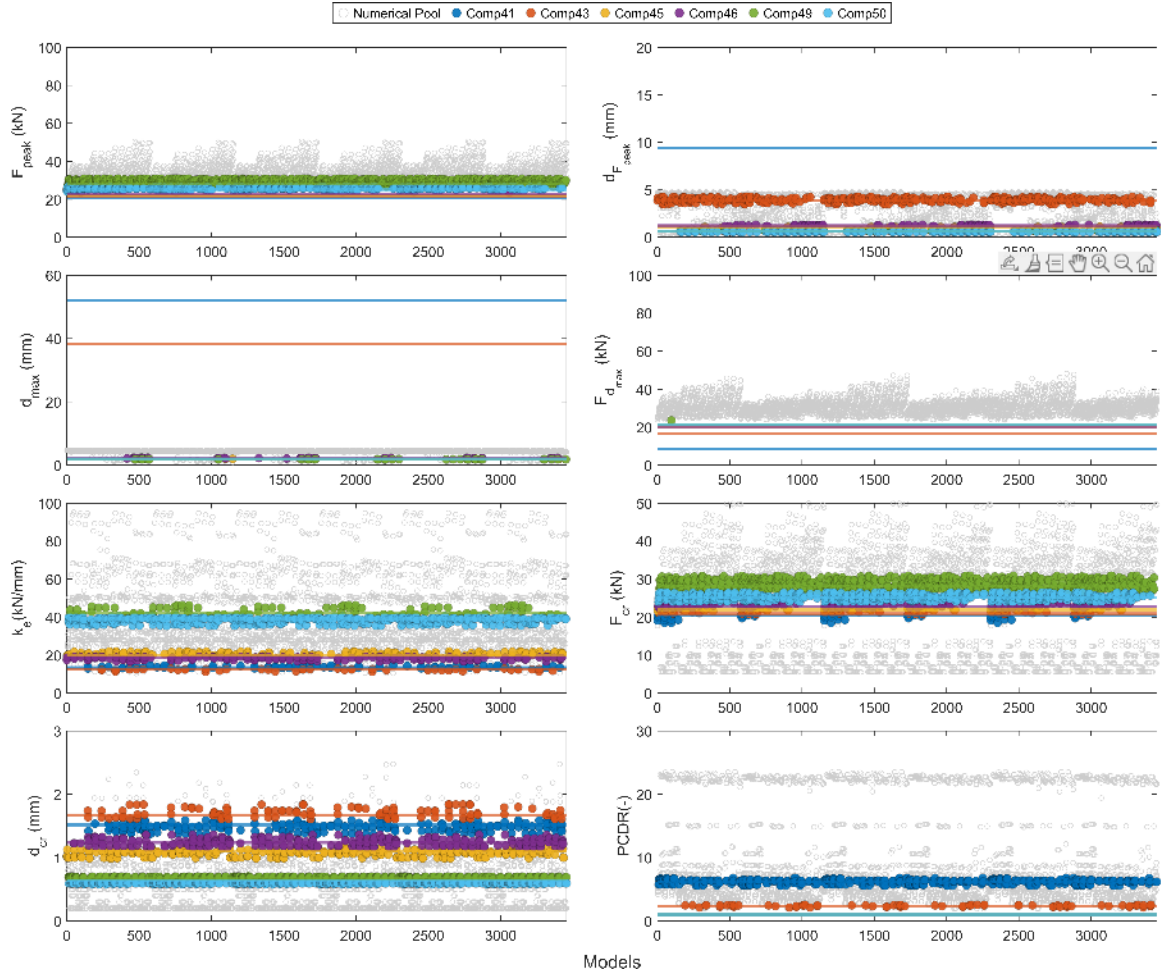


**Figure 6: Models with a tolerance of 10% relevant output parameters obtained from clay and calcium-silicate walls in-plane testing**

Table 3 summarises the filtered models from the numerical response pool highlighting the closest matches for each experiment. The second and third columns indicate the number and identity of the parameters whose numerical values simultaneously fall within the predefined tolerance range of 10% compared to experimental ones. The fourth column reports the number of models satisfying all these conditions. The last two columns present the total number of models that satisfy at least one parameter's tolerance threshold and the associated parameter set considered during the evaluation.

**Table 3. Summary of numerical models that fall within the threshold for each test.**

Experiment ID	Max No. parameter	Parameters	No. models	At least 1 parameter	No. models
Comp41	3	$k_e$ , $F_{cr}$ , $d_{cr}$	19	$k_e$ , $F_{cr}$ , $d_{cr}$ , PCDR	959
Comp43	4	$k_e$ , $F_{cr}$ , $d_{cr}$ , $d_{Fpeak}$	3	$k_e$ , $F_{cr}$ , $d_{cr}$ , $d_{Fpeak}$ , $F_{peak}$ , PCDR	747
Comp45	3	$k_e$ , $F_{cr}$ , $d_{cr}$	47	$k_e$ , $F_{cr}$ , $d_{cr}$ , $d_{Fpeak}$ , $F_{peak}$ , $d_{max}$	998
Comp46	4	$k_e$ , $F_{cr}$ , $d_{cr}$ , $F_{peak}$	13	$k_e$ , $F_{cr}$ , $d_{cr}$ , $d_{Fpeak}$ , $F_{peak}$ , $d_{max}$	1077
Comp49	4	$k_e$ , $F_{cr}$ , $d_{cr}$ , $F_{peak}$	38	$k_e$ , $F_{cr}$ , $d_{cr}$ , $d_{Fpeak}$ , $F_{peak}$ , $d_{max}$ , $F_{dmax}$	2475
Comp50	4	$k_e$ , $F_{cr}$ , $d_{cr}$ , $F_{peak}$	3	$k_e$ , $F_{cr}$ , $d_{cr}$ , $d_{Fpeak}$ , $F_{peak}$ , $d_{max}$	2121

Table 4 presents the parameter combinations that has the most favorable Experimental Agreement Criteria (EAC), which corresponds to the lowest mean RMSE calculated considering the models within 10% threshold for each experiment. The EAC values vary across experiments, with Model 0101 achieving the closest match between the model and test Comp45, representing a clay URM wall. The lowest, 0.82 of EAC, was achieved with Model 0112 for the CaSi URM wall. It is noted that equal weights for each output parameter were considered while computing the EAC (minimum mean RMSE) value. Compressive strength ( $f_c$ ) appears to be the least relevant input parameter for the output parameters considered in Table 3, as changes in this parameter had minimal impact on the model's performance in comparison to the other parameters. Regarding Young's modulus ( $E$ ), its range varies significantly between the materials tested. For clay masonry,  $E$  ranges from 2000 MPa to 5000 MPa, while for CaSi masonry, it ranges from 4000 MPa to 9000 MPa. This difference reflects the distinct material properties of the two types of masonry, which likely influence the overall stiffness and response to loading.

Overall, this table emphasises the need to carefully balance the model's numerical accuracy (minimizing RMSE) with the physical understanding of the system. The goal is to find parameter combinations that not only provide a low EAC but also align with the expected material and structural behaviour. It is important to note that the study is still in its early stages, with a focus on a limited set of output parameters. While the findings are promising, they should be interpreted within the context of these initial constraints. Future work will need to expand the scope by considering additional critical factors, such as energy dissipation, cyclic behaviour, and damage mechanisms, which are vital to understanding the full seismic performance of the models.

**Table 4. Parameter combinations with the highest EAC for each test**

Experiment ID	Model ID	TSCM	$E$ (MPa)	$f_t$ (MPa)	$p$ (-)	$G_{ft}$ (N/mm)	$f_c$ (MPa)	EAC
Comp41	0673	Rotating	2000	0.10	0.20	0.005	5	0.77
Comp43	0241	Fixed	2000	0.10	0.20	0.010	5	1.00
Comp45	0101	Fixed	5000	0.10	0.20	0.005	5	0.75
Comp46	0053	Fixed	5000	0.10	0.15	0.005	5	0.78
Comp49	0112	Fixed	9000	0.20	0.20	0.005	5	0.82
Comp50	0692	Rotating	4000	0.25	0.20	0.005	5	0.99

## CONCLUDING REMARKS AND FUTURE WORK

This study presents a preliminary analysis of the in-plane seismic response of unreinforced clay and calcium silicate masonry walls, based on a series of experimental and numerical investigations. Following the experimental phase, a semi-automated numerical analysis was performed to model the seismic behaviour of the masonry walls. The numerical part of the study included a parametric analysis of 3,456 models, referred to as permutations, from which a pool of numerical responses was extracted. These responses were analysed using correlation techniques and tree-based models to identify key parameters that significantly influenced the output. The results of the numerical analysis were then compared with the experimental data.

The study reveals that different material properties could lead to similar output responses, suggesting that there is not always a direct, one-to-one relationship between material properties and experimental results. However, this analysis was limited to a specific set of input and output parameters. A key challenge encountered in this study was the need for a clearer bridge between the numerical modelling phase and the experimental comparison. While the correlation analysis and tree-based model provided useful insights, future work will be required to refine the connection between these two steps, ensuring a more cohesive workflow between the numerical and experimental analyses.

Overall, this preliminary study offers promising insights into the numerical models, while also highlighting the need for further refinement of the methodology. Future research will aim to expand the parameter set and develop a more integrated approach, incorporating additional parameters and improving the linkage between numerical and experimental results, such as crack patterns, energy dissipation.

## ACKNOWLEDGEMENTS

This research and conference participation of the authors is financially supported by Instituut Mijnbouwschade Groningen (IMG).

## REFERENCES

- [1] D’Altri, A.M., Sarhosis, V., Milani, G., Rots, J., Cattari, S., Lagomarsino, S. et al. (2019) Modeling Strategies for the Computational Analysis of Unreinforced Masonry Structures: Review and Classification. *Archives of Computational Methods in Engineering*, Springer Netherlands. 1–61. <https://doi.org/10.1007/s11831-019-09351-x>
- [2] Parisse, F., Cattari, S., Marques, R., Lourenço, P.B., Magenes, G., Beyer, K. et al. (2021) Benchmarking the seismic assessment of unreinforced masonry buildings from a blind prediction test. *Structures*, 31, 982–1005. <https://doi.org/10.1016/j.istruc.2021.01.096>
- [3] Messali, F., Pari, M., Esposito, R., Rots, J.G. and den Hertog, D. (2018) Blind prediction of a cyclic pushover test on a two-storey masonry assemblage: a comparative study. *Proceedings of the 16th European Conference on Earthquake Engineering*, Thessaloniki.
- [4] Cattari, S. and Magenes, G. (2022) Benchmarking the software packages to model and assess the seismic response of unreinforced masonry existing buildings through nonlinear static analyses [Internet]. *Bulletin of Earthquake Engineering*. Springer Netherlands. <https://doi.org/10.1007/s10518-021-01078-0>
- [5] Tomić, I., Penna, A., Dejong, M.J., Butenweg, C., Correia, A., Candeias, P.X. et al. (2024) Shake-table testing of a stone masonry building aggregate: Overview of blind prediction study. *Bulletin of Earthquake Engineering*,.
- [6] Aşıkoğlu, A., Vasconcelos, G., Lourenço, P.B. and Pantò, B. (2020) Pushover analysis of unreinforced irregular masonry buildings: Lessons from different modeling approaches. *Engineering Structures*, 218. <https://doi.org/10.1016/j.engstruct.2020.110830>
- [7] Korswagen, P.A., Longo, M. and Rots, J.G. (2020) Calcium silicate against clay brick masonry: an experimental comparison of the in-plane behaviour during light damage. *Bulletin of Earthquake Engineering*, Springer Netherlands. 18, 2759–81. <https://doi.org/10.1007/s10518-020-00803-5>
- [8] Korswagen, P.A. (2024) Quantifying the probability of light damage to masonry structures: An exploration of crack initiation and progression due to seismic vibrations on masonry buildings with existing damage. Delft University of Technology, [Delft]. <https://doi.org/10.4233/uuid:e56827d2-c821-4547-922e-ea24bd748e68>
- [9] DIANA FEA. (2025) DIANA Finite Element Analysis (v. 10.10). Denise F, and Jonna M, editors. DIANA FEA BV, The Hague, The Netherlands.
- [10] Vecchio, F.J. and Collins, M.P. (1986) The modified compression-field theory for reinforced concrete elements subjected to shear. *ACI J*, 83, 219–31.
- [11] MathWorks. (2023) MATLAB R2023b. The Mathworks Inc, Natick, Mass.